Expanding Selfsimilar Solutions of a Crystalline Flow with Applications to Contour Figure Analysis

Hidekata Hontani [a], Mi-Ho Giga [b], Yoshikazu Giga [b], Koichiro Deguchi [c]

[a] *Department of Informatics, Yamagata University, Yonezawa, Yamagata, 992-8510, Japan*

[b] *Department of Mathematics, Hokkaido University, Sapporo, Hokkaido, 060-0810, Japan*

[c] *Department of System Information Sciences, Graduate School of Tohoku University, Sendai, 980-8579, Japan*

Abstract

A numerical method for obtaining a crystalline flow starting from a general polygon is presented. A crystalline flow is a polygonal flow and can be regarded as a discrete version of a classical curvature flow. In some cases, new facets may be created instantaneously and their facet lengths are governed by a system of singular ordinary differential equations (ODEs). The proposed method solves the system of the ODEs numerically by using expanding selfsimilar solutions for newly created facets. The computation method is applied to a multi-scale analysis of a contour figure.

Key words: crystalline flow, selfsimilar solutions, evolving polygon, multi-scale analysis

1 Introduction

A curvature flow is widely used for a multi-scale analysis of a contour figure in an image[1–7]. A curvature flow is a family of evolving contours, in which every point of the contour moves toward its normal direction with the velocity that is determined by the curvature. Figure 1 shows an example of a curvature flow, in which the normal velocity is equal to the curvature. This flow is called a curve shortening flow. As a contour evolves, local details in the contour are smoothed out, and its shape becomes close to a circle. Many methods for a multi-scale analysis specify a shape component from a given contour and

find each component's size by observing how the contour shape changes in the curve shortening flow, and describe the hierarchical structure of a given contour figure.

In many cases, a contour figure in an image is described as a polygon. In a curve shortening flow, it is proved that any given simple polygon becomes an analytic curve immediately after it starts evolving. There have been proposed several methods for computing the flow, and those methods usually describe an evolving smooth contour in a discrete way.

The Gaussian-based method[4], for example, describes an evolving contour figure by a set of points that are equally spaced in the contour. The coordinates of the ith point is represented as $(x(i\Delta), y(i\Delta))$ where Δ denotes the interval between adjacent points. The method iterates two processes: (i) smoothing both x and y with a small scale Gaussian filter, and (ii) resampling the resulted contour at equal intervals after the smoothing. The resampling process is needed because the arc length changes as the contour evolves. This resampling process deforms the shape of the represented contour figure slightly at each iteration step. In addition, the interval Δ changes at each iteration because Δ must aliquot of the total peripheral length, but it is not realizable. Many multi-scale methods track a point in a given contour through the evolution. The resampling process makes it difficult to track each point in the contour straightforwardly.

A level set method[8–10] is a powerful tool for obtaining an evolving interface. The method represents an evolving interface as the zero level set of an auxiliary function ϕ. For example, an evolving contour in the x-y plane is represented as the zero level set of the evolving function $\phi(x, y; t)$. To compute the curve shortening flow, we only need to solve the level set equation $\phi_t + \kappa|\nabla\phi| = 0$. Because no arc length parameter along the contour is needed for computation, no resampling along the contour is needed. Moreover, the method can compute an evolving interface even if its topology changes as it evolves. In the computation, though, the function ϕ is discretely represented on fixed pixels, and finite difference operators are used for computing the spatial derivatives. The operators' width is usually two or three pixels. If there exists a small part in the evolving contour that is comparable to the operators' width, then, the computed values do not approximate well the spatial derivatives. This inaccuracy causes a serious problem to compute the accurate value

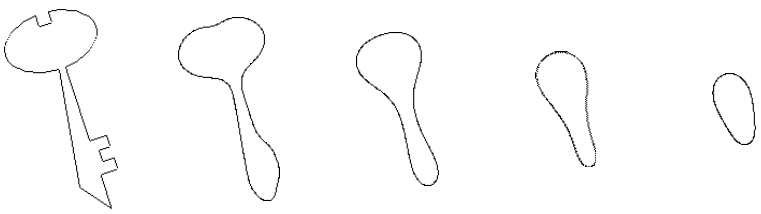

Fig. 1. An example of a curve shortening flow

of the curvature κ. Unless we know the accurate value of κ, it is, for example, difficult to choose inflection point of an evolving curve, which is important in a multi-scale contour figure analysis (see e.g. [1,2,4–7])

In [11] and [12], a crystalline flow is proposed to analyze motion of crystals. The crystalline flow is a special family of evolving polygons. It can be regarded as a discrete version of a curvature flow. In an evolving process of the crystalline flow, a given polygon remains polygonal through the evolving process, each facet (side) of evolving contour moves keeping its normal direction, and every corner in the contour moves at least C^1 in time (provided that no facets disappear). These features help to track each facet through the evolving process, so that the flow is useful for the multi-scale analysis. The velocity is determined by the non-local curvature, which depends on the length of the facet. Polygons are well represented in a discrete manner. Different from a classical curvature flow, it is easy to compute the accurate value of non-local curvature, and to obtain the crystalline flow if an appropriate initial polygon is given.

The crystalline flow proposed in [11] and [12] restricted initial polygonal contour. In [13] and [14], a level set formulation was extended to handle some family of non-local curvature flow including a crystalline flow. Moreover, any polygon can be taken as an initial contour of a crystalline flow. In some cases, new facets are created at corners of a given polygon instantaneously. Once new facets are created, then, no new facet is not created any more, and the number of facets decreases monotonically, as time increases unless evolving polygon degenerates. Recently, a system of singular ordinary differential equations of their facet lengths has been studied to handle new facets creation[15]. If the speeds of both facets bounding newly created facets are zero, then these new facets expand selfsimilarly, which are obtained by solving an algebraic equation[15].

In this paper, we present a numerical method for solving the system of ODEs to obtain a crystalline flow from *arbitrary* given polygon (see also [16]). A numerical length of each new facet is systematically calculated. The proposed method enables us to use any simple and convex polygon as the Wulff shape, which controls the nonlocal curvature of each facet. As mentioned above, a crystalline flow has useful features for a multi-scale analysis of a contour figure. In fact, in [17] the first and the last authors first applied a crystalline flow to a multi-scale contour figure analysis, so that the method extracts dominant corners from a given polygon. However, the method in [16] did not create new facets systematically. In this paper, the length of each new facet is approximated by expanding selfsimilar solutions (obtained in [15]).

This paper is organized as follows: In Section 2, we outline mathematical backgrounds of a crystalline flow with expanding selfsimilar solutions, which may

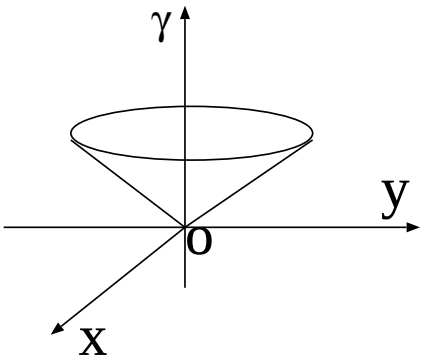

Fig. 2. Interfacial energy density γ

appear as newly created facets. In Section 3, we present a numerical method for computing a crystalline flow. Section 4 and 5 show some experimental results and conclusions respectively.

2 Crystalline Flow

2.1 Weighted Curvature Flow

First, we recall the notion of the weighted curvature. Let γ be a continuous, convex function on $\boldsymbol{R}^2$ which is positively homogeneous of degree one, i.e., $\gamma(\lambda \boldsymbol{p}) = \lambda\gamma(\boldsymbol{p})$ for all $\boldsymbol{p} \in \boldsymbol{R}^2$, $\lambda > 0$. Assume that $\gamma(\boldsymbol{p}) > 0$ for $\boldsymbol{p} \neq 0$. For a moment assume that γ is smooth (except the origin). Figure 2 shows an example of the graph of $\gamma(\boldsymbol{p})$. For an oriented curve S with the orientation $\boldsymbol{n}$, which is a unit normal, we call $\Lambda_\gamma(\boldsymbol{n}) = -\mathrm{div}(\boldsymbol{\xi}(\boldsymbol{n}))$ the *weighted curvature* of S in the direction of $\boldsymbol{n}$, where $\boldsymbol{\xi} = \nabla\gamma$. We note that the weighted curvature of S is the first variation of $I(S)$ with respect to a variation of the area enclosed by S ; here $I(S)$ is defined by

$$I(S) = \int_S \gamma(\boldsymbol{n})\,\mathrm{d}s, \tag{1}$$

where ds denotes the line element; $I(S)$ is called the *interfacial energy* with an *interfacial energy density* γ. We recall that the Wulff shape defined by

$$W_\gamma = \bigcap_{|\boldsymbol{m}|=1} \{\boldsymbol{x} \in \boldsymbol{R}^2; \boldsymbol{x} \cdot \boldsymbol{m} \leq \gamma(\boldsymbol{m})\}$$

is the unique minimizer of $I(S)$ among all S whose enclosed area is the same as W_γ (see e.g. [18]). If $\gamma(\boldsymbol{p}) = |\boldsymbol{p}|$, then $I(S)$ is equal to the total peripheral length of S, Λ_γ is the usual curvature, and W_γ is nothing but a unit disk. For

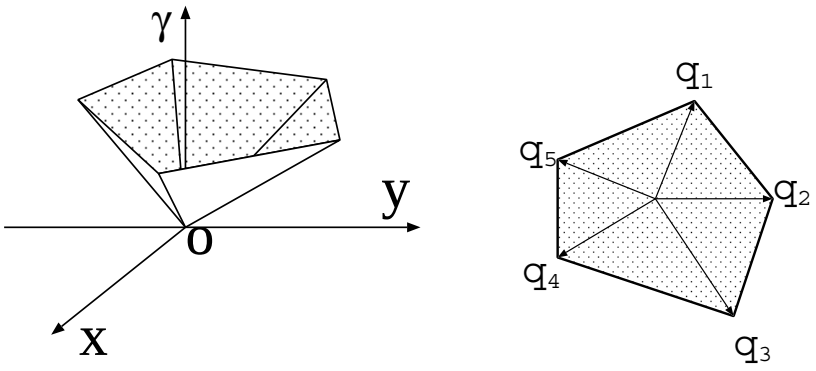

Fig. 3. Crystalline energy density, and its Frankγ

any γ the weighted curvature of ∂W_γ always equals -1, so W_γ plays the role of a unit disk for the usual curvature.

We consider a motion of an evolving curve Γ_t governed by the *anisotropic curvature flow equation* of the form

$$V = \Lambda_\gamma(\boldsymbol{n}) \tag{2}$$

on Γ_t, where V denotes the normal velocity of $\{\Gamma_t\}$ in the direction of $\boldsymbol{n}$. When $\gamma(\boldsymbol{p}) = |\boldsymbol{p}|$, equation (2) becomes the curve shortening equation.

There are several methods to track evolution of Γ_t; one of a typical method is the level-set method (see [8–10,19]). If γ is C^2 except the origin, global unique solvability for (2) is established by [10] (see also [20]). However, when γ has corners, conventional notion of a solution including viscosity solutions does not apply to (2).

If Frank diagram of γ :

$$\text{Frank}\gamma = \{\boldsymbol{p} \in \mathbf{R}^2; \gamma(\boldsymbol{p}) \leq 1\}$$

is a convex polygon, γ is called a *crystalline energy (density)* (see Fig.3), and a notion of solution for (2) is proposed by [11] and [12] independently by restricting $\{\Gamma_t\}$ as a special family of evolving polygonal curves called admissible. Even for more general γ with corners not necessarily crystalline energy, the level-set approach for (2) and more general equations is successfully extended by [14] (see also [13]), although the problem has nonlocal nature. They introduced a new notion of solution consistent with that in [11] and [12], and proved the global unique solvability at least for a *general* initial simple curve (not necessarily admissible).

2.2 Crystalline Flow

Here and hereafter we assume that γ is a crystalline energy, i.e., Frank γ is a convex M-polygon. In this section we introduce an evolving polygonal curve called a crystalline flow governed by (2). To track such an evolving polygon, we shall derive a system of ordinary differential equations (ODEs) for the length of sides (facets) of the polygon. For this purpose we need to prepare several notions.

Let $\boldsymbol{q}_i$ $(i = 1, \ldots, M)$ be vertices of Frankγ as shown in Fig3. We call a simple polygonal curve S as an *essentially admissible crystal* if the outward unit normal vector $\boldsymbol{n}$ and $\hat{\boldsymbol{n}}$ of any adjacent segments (facets) of S satisfy

$$\frac{(1-\lambda)\boldsymbol{n} + \lambda\hat{\boldsymbol{n}}}{|(1-\lambda)\boldsymbol{n} + \lambda\hat{\boldsymbol{n}}|} \notin \mathcal{N} \tag{3}$$

for any $\lambda \in (0,1)$, where $\mathcal{N} = \{\boldsymbol{q}_i/|\boldsymbol{q}_i|;\ i = 1, \ldots, M\}$. Let J be a time interval. We say that a family of polygon $\{S(t)\}_{t\in J}$ is an *essentially admissible evolving crystal* if $S(t)$ is an essentially admissible crystal for all $t \in J$ and each corner moves continuously differentiably in time. These conditions imply that the orientation of each facet is preserved in J. By definition $S(t)$ is of the form $S(t) = \cup_{j=1}^{r} S_j(t)$ where $S_j(t)$ is a maximal, nontrivial, closed segment and its unit outward normal vector is $\boldsymbol{n}_j$. Here we number facets clockwise. Then we obtain a transport equation for $L_j(t)$ which is the length of $S_j(t)$:

$$\frac{\mathrm{d}L_j(t)}{\mathrm{d}t} = (\cot\psi_j + \cot\psi_{j+1})V_j - \frac{1}{\sin\psi_j}V_{j-1} - \frac{1}{\sin\psi_{j+1}}V_{j+1} \tag{4}$$

for $j = 1, \ldots, r$; index j is considered modulo r. Here $\psi_j = \theta_j - \theta_{j-1}$ (modulo 2π) with $\boldsymbol{n}_j = (\cos\theta_j, \sin\theta_j)$, and V_j denotes the normal velocity of $S_j(t)$ in the direction of $\boldsymbol{m}_j$.

We say that an essentially admissible crystal $\{S(t)\}_{t\in J}$ is a *γ-regular flow* of (2) if

$$V_j(t) = \chi_j \frac{\Delta(\boldsymbol{n}_j)}{L_j(t)} \tag{5}$$

for $j = 1, 2, \ldots, r$. Here $\Delta(\boldsymbol{n}_j) = \tilde{\gamma}'(\theta_j + 0) - \tilde{\gamma}'(\theta_j - 0)$ with $\boldsymbol{n}_j = (\cos\theta_j, \sin\theta_j)$ and $\tilde{\gamma}(\theta) = \gamma(\cos\theta, \sin\theta)$. We note that $\Delta(\boldsymbol{n}_j)$ is the length of facet of W_γ with outward normal $\boldsymbol{n}_j$ if $\boldsymbol{n}_j \in \mathcal{N}$ (see Fig.4), otherwise $\Delta(\boldsymbol{n}_j) = 0$. The quantity χ_j is called a transition number, and takes $+1$ (resp.-1) if the j-th facet is concave (resp. convex) in the direction of $\boldsymbol{n}_j$, otherwise $\chi_j = 0$.

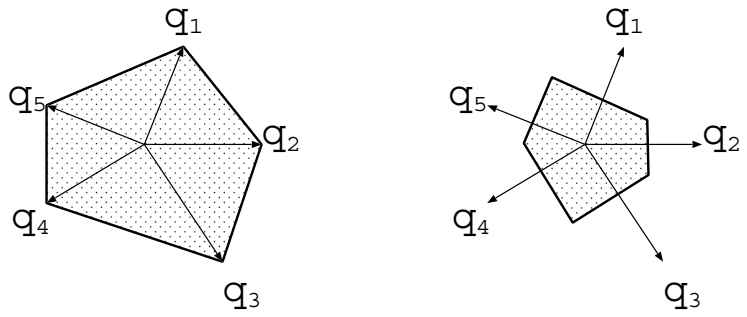

Frankγ Wulff shape

Fig. 4. Frankγ and corresponding Wulff shape. Each facet of the Wulff shape has the length $\Delta(\boldsymbol{m}_i)$, where $\boldsymbol{m}_i = \boldsymbol{q}_i/|\boldsymbol{q}_i|$.

We call the quantity $\Lambda_j \equiv \chi_j \Delta(\boldsymbol{n}_j)/L_j(t)$ as a *nonlocal weighted curvature* of the j-th facet with respect to γ. (We use the convention that $1/L_j(t) = 0$ if $L_j(t) = \infty$.) Thus we get a system of ODEs (4) and (5) for $L_j(t)$'s. For a moment we assume that $S(0)$ is an essentially admissible closed curve.

A fundamental theory of ODE yields the (local in time) unique solvability of (4) and (5). Unless $S(t)$ shrinks to a point, self-intersects, or develops degenerate pinching at most two consecutive facets with zero nonlocal weight curvatures may disappear (i.e., the length of a facet tends to zero) at some time T_*. However, $S(T_*)$ remains essentially admissible, so that we can continue calculating the ODE system (5),(6) for $t > T_*$ starting with initial data $S(T_*)$ (see [12,13]).

We say that $\{S(t)\}_{t\in J}$ is a *crystalline flow* with initial data $S(0)$, if there is some $t_0 = 0 < t_1 < t_2 < \cdots < t_l$, such that $\{S(t)\}_{t\in J_h}$ is a γ-regular flow for $J_h = [t_h, t_{h+1})$ with initial data $S(t_h)$ $(h = 0, 1, \ldots, l-1)$, and $S(t) \to S(t_{h+1})$ in the sense of the Hausdorff distance topology as $t \uparrow t_{h+1}$ and some facets disappear at t_{h+1} $(h = 0, 1, \ldots, l-2)$. By a similar argument as in [13], we see that a crystalline flow $\{S(t)\}_{t\in J}$ starting with essentially admissible closed curve $S(0)$ shrinks to a point and does not intersect nor develop degenerate pinching. A crystalline flow $\{S(t)\}_{t\in J}$ agrees with a solution by level-set approach for (2) introduced in [14], by a similar argument as in [13]. The discussion in [13] is for an admissible evolving crystal but it is easy to extend to an essentially admissible evolving crystal. For convenience we recall the notion of an admissible evolving crystal. An essentially admissible crystal S is called an *admissible crystal* if the outward unit normal vector $\boldsymbol{m}$ of each segment of S belongs to $\mathcal{N}$. We say $\{S(t)\}_{t\in J}$ is an *admissible evolving crystal* if $S(t)$ is an admissible crystal for each $t \in J$.

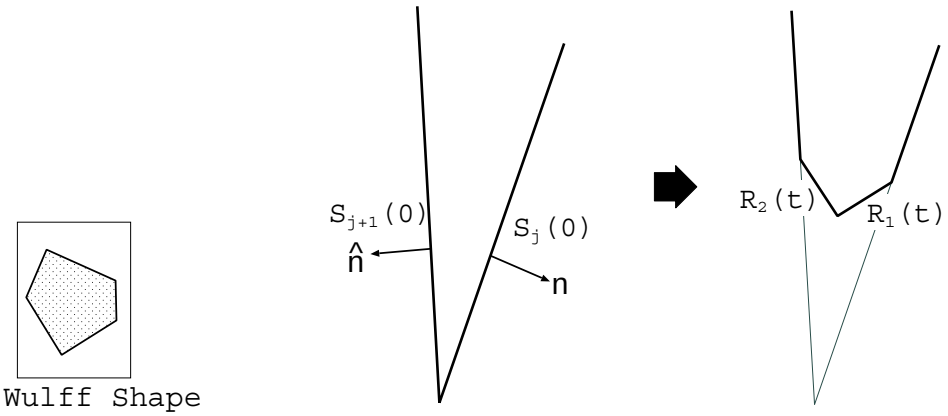

Fig. 5. Creation of a set of new facets. All facets with orientation in $\mathcal{M}$ is expected to be created between $S_j(0)$ and $S_{j+1}(0)$ just after $t = 0$. It should be noted that the length of each new facet should satisfy the ODE system of (4) and (5).

2.3 General polygonal initial curve

In the previous section we restricted an initial curve to an essentially admissible crystals. Here we shall focus on a simple, closed, polygonal initial curve $S(0)$, which is not necessarily an essentially admissible crystal. In [14], it is shown that there exists a unique level-set flow (solution) for (2) with a crystalline energy γ starting with a general polygonal initial curve. However, it is not clear a priori whether or not the solution is described by an ODE system, since new facets whose orientation belongs to $\mathcal{N}$ are expected to be created instantaneously at the place where the property (3) is violated on $S(0)$. Moreover, it is not clear how to solve the expected ODE system since it is singular at newly created facets. In this section we give a heuristic argument to solve such a singular ODE system.

Let $\boldsymbol{n}$ and $\hat{\boldsymbol{n}}$ be the orientation of any adjacent facets $S_j(0)$ and $S_{j+1}(0)$ of $S(0)$. If

$$\mathcal{M} \equiv \left\{ \frac{(1-\lambda)\boldsymbol{n} + \lambda\hat{\boldsymbol{n}}}{|(1-\lambda)\boldsymbol{n} + \lambda\hat{\boldsymbol{n}}|} \in \mathcal{N} \ ; \ 0 < \lambda < 1 \right\}$$

is not the empty set, all facets (say, $R_1(t), \ldots, R_n(t)$, numbered clockwisely) with orientation in $\mathcal{M}$ is expected to be created between $S_j(0)$ and $S_{j+1}(0)$ just after $t = 0$, so that the transition number of each $R_i(t)$ is 1 (resp. -1) for small $t > 0$ if the bounded polygon enclosed by $S(0)$ is concave (resp. convex) near $S_j(0) \cap S_{j+1}(0)$ (see Fig.5). By inserting these newly created facets, our solution $S(t)$ becomes essentially admissible instantaneously. This observation should be justified by approximating $S(0)$ by essentially admissible crystals from inside and from outside with comparison principle[14].

For a given initial polygon $S(0)$ one is able to find the place, the orientation and the transition number of the all facets that are expected to be newly created at initial time. For later convenience, we shall re-number clockwisely all facets of $S(0)$ and all facets that are expected to be created at $t = 0$, i.e., the length of a newly created facet equals 0 at $t = 0$. Then the expected ODE system for a simple, closed, polygonal initial curve $S(0)$ again becomes (4) and (5) ; however, the initial data $L_j(0)$ may be 0. The ODE system is of the form

$$\frac{\mathrm{d}L_j(t)}{\mathrm{d}t} = \frac{\tilde{p}_j}{L_j(t)} + \frac{\tilde{q}_{j-1}}{L_{j-1}(t)} + \frac{\tilde{r}_{j+1}}{L_{j+1}(t)}, \tag{6}$$

where $\tilde{p_j} = (\cot\psi_j + \cot\psi_{j+1})\chi_j\Delta(\boldsymbol{n}_j)$, $\tilde{q}_{j-1} = -\chi_{j-1}\Delta(\boldsymbol{n}_{j-1})/\sin\psi_j$, and $\tilde{r}_{j+1} = -\chi_{j+1}\Delta(\boldsymbol{n}_{j+1})/\sin\psi_{j+1}$ for $j = 1, \ldots, r'$; index j is considered modulo r'. Here numbers $\tilde{p}_j, \tilde{q}_j, \tilde{r}_j$ are determined uniquely by (4) and (5), since the transition number and the orientation of a newly created facet are known.

To solve the equation (6) we consider Puiseux series

$$L_j(t) = \sum_{k=0}^{\infty} a_{jk} t^{k/2}, \tag{7}$$

with real number a_{jk} . Clearly, for j with $L_j(0) = 0$ the coefficient a_{j0} must be zero. Suppose that n consecutive facets, say $S_1(t), \ldots, S_n(t)$ are created at $t = 0$, i.e. $L_1(0) = \ldots = L_n(0) = 0$ and $L_0(0)$, $L_{n+1}(0) > 0$. We plug (7) into (6) and multiply $t^{1/2}$ with the both sides of (6). Comparing both sides we observe that all coefficients are determined. The first coefficients $\{a_{j1}\}_{j=1}^n$ have a significant meaning. If the nonlocal curvature of $S_0(0)$ and $S_{n+1}(0)$ equal zero, then $L_j(t) = a_{j1}t^{1/2}$ for $j = 1, \ldots, n$ exactly solves the ODE system (6) with $j = 1, \ldots, n$ (as long as both $S_0(t)$ and $S_{n+1}(t)$ exist), since it is decoupled from the whole system (6) with $j = 1, \ldots, r'$ by the fact $\tilde{q}_0 = 0 = \tilde{r}_{n+1}$. In this case the solution $\{a_{j1}\}_{j=1}^n$ represents a selfsimilar expanding solution of the problem in the next section.

2.4 Selfsimilar expanding solutions

Let $\{S(t)\}_{t>0}$ be an essentially admissible evolving crystal of the form $S(t) = \cup_{j=0}^{n+1} S_j(t)$ with nonparallel half lines $S_0(t)$ and $S_{n+1}(t)$. We say that $\{S(t)\}_{t>0}$ is *selfsimilar* if there exists an essentially admissible crystal S_* such that

$$S(t) = t^{1/2}S_* = \{t^{1/2}\boldsymbol{x}; \boldsymbol{x} \in S_*\}, \quad t > 0.$$

If $\{S(t)\}_{t>0}$ solves (6), we call $\{S(t)\}_{t>0}$ a *selfsimilar expanding solution* of (2). By definition $S(+0) = \lim_{t\downarrow 0} S(t)$ consists of two (nonparallel) half lines emanated from the origin. We also observe that $\cup_{j=1}^{n} S_j(t)$ is admissible for all $t > 0$ and that the transition number of $S_j(t)$ is independent of $j = 1, \ldots, n$ and $t > 0$; it must be either -1 or $+1$. It turns out that $\{S(t)\}_{t>0}$ is a selfsimilar expanding solution if and only if the length $L_j(t)$ of $S_j(t)$ $(j = 1, \ldots, n)$ solves the ODE system (6) for $t > 0$ and for $j = 1, \ldots, n$ with $\tilde{q}_0 = 0 = \tilde{r}_{n+1}$. Note that a_{j1} of $L_j(t) = a_{j1}t^{1/2}$ represents the length of j-th facet of S_* for $j = 1, \ldots, n$.

Theorem 1 *For a given oriented closed cone C (with connected interior) there exists a unique selfsimilar expanding solution $S(t)$ such that $S(+0)$ agrees with the boundary of C (see [15]).*

From ODE system (6) we see that this problem is equivalent to the unique solvability of algebraic equation

$$\begin{bmatrix} a_n \\ a_{n-1} \\ a_{n-2} \\ \vdots \\ a_2 \\ a_1 \end{bmatrix} = 2 \begin{bmatrix} \tilde{p}_n & \tilde{q}_{n-1} & & & & \\ \tilde{r}_n & \tilde{p}_{n-1} & \tilde{q}_{n-2} & & 0 & \\ & \tilde{r}_{n-1} & \tilde{p}_{n-2} & \tilde{q}_{n-3} & & \\ & & \ddots & \ddots & \ddots & \\ & 0 & & \tilde{r}_3 & \tilde{p}_2 & \tilde{q}_1 \\ & & & & \tilde{r}_2 & \tilde{p}_1 \end{bmatrix} \begin{bmatrix} 1/a_n \\ 1/a_{n-1} \\ 1/a_{n-2} \\ \vdots \\ 1/a_2 \\ 1/a_1 \end{bmatrix} \tag{8}$$

for $a_j = a_{j1} (j = 1, 2, \ldots, n)$. We solved this equation by a method of continuity while we proved the uniqueness of a solution by a geometric observation[15].

3 Numerical Method for Obtaining a Crystalline Flow

In this section, we describe a numerical method for obtaining a crystalline flow starting from a given polygon that is not necessarily an essentially admissible crystal. Using the Euler method, we compute the approximated solution of the system of (4) and (5). If the given polygon is not essentially admissible, our method firstly creates new facets. When the new facets are created, the length of any facet in a given polygon is not updated. After the new facets are created, then we update the lengths of all facets to compute the approximated solution.

For each adjacent facets with orientation $\boldsymbol{m}$ and $\hat{\boldsymbol{m}}$ of the initial polygon, if $\mathcal{M} \neq \emptyset$ then all facets with orientation in $\mathcal{M}$ should be newly created instantaneously, so that the given polygon becomes essentially admissible instantaneously. Once the polygon becomes essentially admissible, no new facet is needed to be created.

Given a non essentially admissible polygon, the method creates new facets at first time. For creating new facets, we should numerically calculate the solution of (8) in order to obtain the lengths of them. Let the time step be denoted as Δt. We set the length of each new facet to $a_j\sqrt{\Delta t}$, where a_j is a numerical solution of (8).

To solve (8) numerically, as in [15] we rewrite (8) with $\alpha_j = 1/a_j$:

$$\begin{bmatrix} 1/\alpha_n \\ 1/\alpha_{n-1} \\ \vdots \\ 1/\alpha_2 \\ 1/\alpha_1 \end{bmatrix} = H_n \begin{bmatrix} \alpha_n \\ \alpha_{n-1} \\ \vdots \\ \alpha_2 \\ \alpha_1 \end{bmatrix}, \text{ where } H_n = \begin{bmatrix} p_n & q_{n-1} & & & \\ r_n & p_{n-1} & q_{n-2} & & 0 \\ & \ddots & \ddots & \ddots & \\ 0 & & r_3 & p_2 & q_1 \\ & & & r_2 & p_1 \end{bmatrix}, \tag{9}$$

where $p_j = 2\tilde{p}_j$, $q_j = 2\tilde{q}_j$, and $r_j = 2\tilde{r}_j$. We introduce extra parameter $s \in [0, 1]$ by replacing H_n by $K_n(s)$ in (9) so that α_j depends on s.

$$K_n(s) = \begin{bmatrix} p_n & sq_{n-1} & & & \\ sr_n & p_{n-1} & sq_{n-2} & & 0 \\ & \ddots & \ddots & \ddots & \\ 0 & & sr_3 & p_2 & sq_1 \\ & & & sr_2 & p_1 \end{bmatrix}. \tag{10}$$

Evidently $[1/\alpha_j(0)] = K_n(0)[\alpha_j(0)]$ can be easily solved, and $\{\alpha_j(1)\}_{j=1}^n$ is the solution of (9): $\alpha_j(0) = 1/\sqrt{p_j}$. Referring the idea of [15], we calculate the numerical solution of (9) using the Newton-Rapson method as follows.

(1) Set $\alpha_j = 1/\sqrt{p_j}$ for initial values of the iteration, where $p_j = 2[\cot\psi_j + \cot\psi_{j+1}]\chi_j\Delta(\boldsymbol{n}_j)$.
(2) Apply the Newton-Rapson method to obtain the numerical solution of α_j.

Finally, we calculate $a_j = 1/\alpha_j$, and set the length of each new facet to $a_j\sqrt{\Delta t}$. Note that $L_j(t) = a_j t^{1/2}$ is the exact solution if the velocities of both facets bounding newly created facets are zero. The polygon obtained by the new facet creation approximates well the solution of the system of (4) and (5) corresponding to $t = \Delta t$.

3.2 Computing Crystalline Flow

As described in the previous subsection, if a given polygon is not essentially admissible, then the new facets are created. The resulted polygon is essentially admissible. Given the Wulff shape and a simple initial polygon, our method computes the solution of the system of (4) and (5) using the Euler method.

(1) Create new facets as described in the previous subsection, if a given initial polygon is not essentially admissible. The length of a facet in the given polygon is not updated in this step.
(2) Update the length of every facet in the polygon as $L_j(t_0 + \Delta t) = L_j(t_0) + \Delta t \cdot \mathrm{d}L_j(t)/\,\mathrm{d}t|_{t=t_0}$.
(3) Iterate step (2) till the polygon becomes convex.

4 Experimental Results

4.1 Computation of a Crystalline Flow

In the first experiment, we used a regular 16-polygon as the Wulff shape, and a sector as an initial contour as shown in Fig(4.1). Let $\boldsymbol{m}_i$ $(i = 1, 2, \cdots, 16)$ denote the outward unit normals of the Wulff shape. We set that the arg $\boldsymbol{m}_i = \pi - \pi(i-1)/8$ (the facet number is counted clockwise). Let S_j denote the jth facet of the initial contour, and $\boldsymbol{n}_j$ $(j = 1, 2, 3, 4)$ be the outward unit normal of S_j. Assume that arg $\boldsymbol{n}_j = \pi - \pi(j-1)/2$. Then, three new facets sprout out at each corner of the square. For example, between S_1 (arg $\boldsymbol{n}_1 = \pi$) and S_2 (arg $\boldsymbol{n}_2 = \pi/2$) of the given square, three facets sprout out of which normals are parallel to $\boldsymbol{m}_2$, $\boldsymbol{m}_3$, and $\boldsymbol{m}_4$, respectively.

In order to obtain the quantities of a_j, we solve next equations that correspond

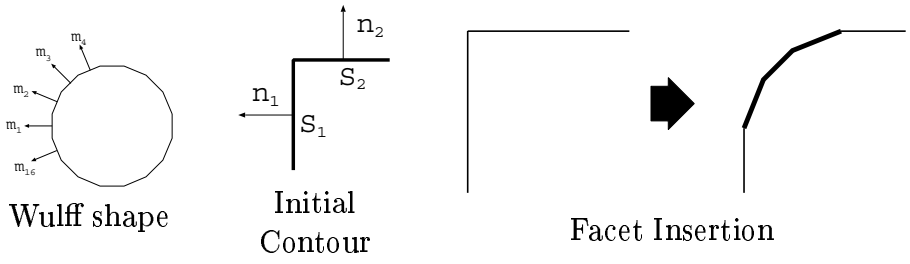

Fig. 6. An example of the Wulff shape and an initial contour. An analytic solution can be calculated in this case. Three new facets are created at the beginning as shown in this figure. It should be noted that the middle facet is shorter than side ones.

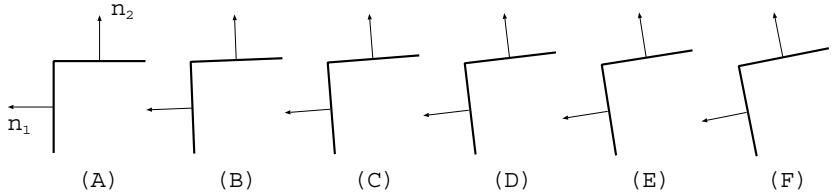

Fig. 7. An example of the set of given rotated sectors. The arguments of $\boldsymbol{n}_1$ are (A) π, (B) $\pi + \pi/80$, (C) $\pi + 2\pi/80$, (D) $\pi + 3\pi/80$, (E) $\pi + 4\pi/80$, and (F) $\pi + 5\pi/80$, respectively.

to (8).

$$\begin{bmatrix} a_4 \\ a_3 \\ a_2 \end{bmatrix} = \begin{bmatrix} p & q & 0 \\ q & p & q \\ 0 & q & p \end{bmatrix} \begin{bmatrix} 1/a_4 \\ 1/a_3 \\ 1/a_2 \end{bmatrix}, \text{ where } p = \frac{4}{\tan(\pi/8)} \text{ and } q = -\frac{2}{\sin(\pi/8)}. \quad (11)$$

Let $\alpha = 1/a_2 = 1/a_4$ and $\beta = 1/a_3$. The equation(11) can be solved analytically:

$$\begin{cases} \alpha = -(p\beta - 1/\beta)/2q, \\ \beta = \left[(p^2+q^2) + \sqrt{(p^2+q^2)^2 - p^2(p^2-2q^2)}\right]^{1/2} / \left[p(p^2-2q^2)\right]^{1/2}. \end{cases} \quad (12)$$

We can calculate the quantities a_j's using $a_2 = a_4 = 1/\alpha$ and $a_3 = 1/\beta$. The values p and q in (12) are known as shown in (11). The values are $a_2 = a_4 \simeq 1.68$ and $a_3 \simeq 1.29$, respectively. Three facets sprout out with symmetric shape in this case. It should be noted that the shape of the set of new facets are not same with the shape of the corresponding part of the Wulff shape. In this case, the middle facet is shorter than the neighbors, in spite that the Wulff shape is regular. Table 1 (A) shows the quantities a_j's of Eq.(11) computed numerically by the method described in Sec.3.1. The computed quantities approximated the solution correctly.

Table 1
Experimental results obtained from the rotated sectors shown in Fig.7. The numerically calculated solutions a_j are shown. The quantity $a_j\sqrt{\Delta t}$ represents the length of the newly created jth facet.

	(A)	(B)	(C)	(D)	(E)	(F)
Arg $\boldsymbol{n}_1$	π	$\pi+\pi/80$	$\pi+2\pi/80$	$\pi+3\pi/80$	$\pi+4\pi/80$	$\pi+5\pi/80$
Arg $\boldsymbol{n}_2$	$\pi/2$	$\pi/2+\pi/80$	$\pi/2+2\pi/80$	$\pi/2+3\pi/80$	$\pi/2+4\pi/80$	$\pi/2+5\pi/80$
a_1	-	5.891	3.924	3.090	2.614	2.303
a_2	1.682	1.464	1.382	1.326	1.286	1.257
a_3	1.287	1.232	1.223	1.225	1.287	1.257
a_4	1.682	1.719	1.806	1.925	2.085	2.303

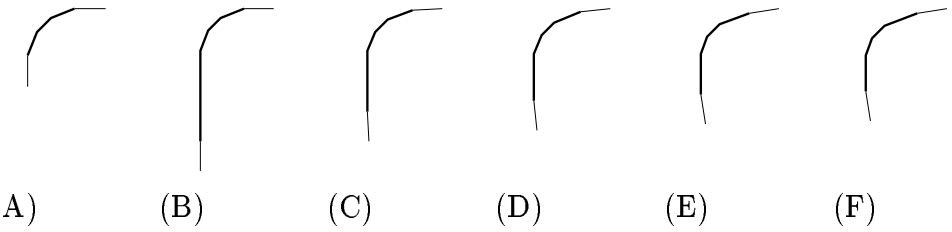

Fig. 8. The shape of new facets that correspond to Fig.7 and Table 1. The thick lines indicate the new facets.

If a given initial contour is rotated, then the shape of new facets changes. We applied the proposed method for each sector shown in Fig. 7. The sector is rotated with increments of $\pi/80$. The length of each new facet is denoted by a_j. Table 1 shows the calculated values of a_j, which correspond to the new facets between S_1 and S_2. If the sector (A) is given, three facets sprout out between S_1 and S_2. On the other hand, the sectors other than (A) are given, because arg $\boldsymbol{n}_2$ < arg $\boldsymbol{m}_1$ < arg $\boldsymbol{n}_1$, four facets sprout out between S_1 and S_2. Figure 8 shows the shape of the new facets. In case that the sector (B) in Fig.7 is given, the normal $\boldsymbol{n}_1$ is almost parallel to the new facet's normal $\boldsymbol{m}_1$, and a_1 is large.

Figure 9 shows some experimental results of crystalline flow. The initial contour is common to all, but the Wulff shape is different. As described before, the Wulff shape plays the role of a unit circle for a classical curve shortening flow. Because the proposed method gives a crystalline flow numerically from a non essentially admissible crystal, any simple and convex polygon can be used for the Wulff shape. A given initial contour becomes essentially admissible instantaneously, no new facet is created. If the Wulff shape is symmetric with respect to some point, then any contour becomes convex in finite time[13].

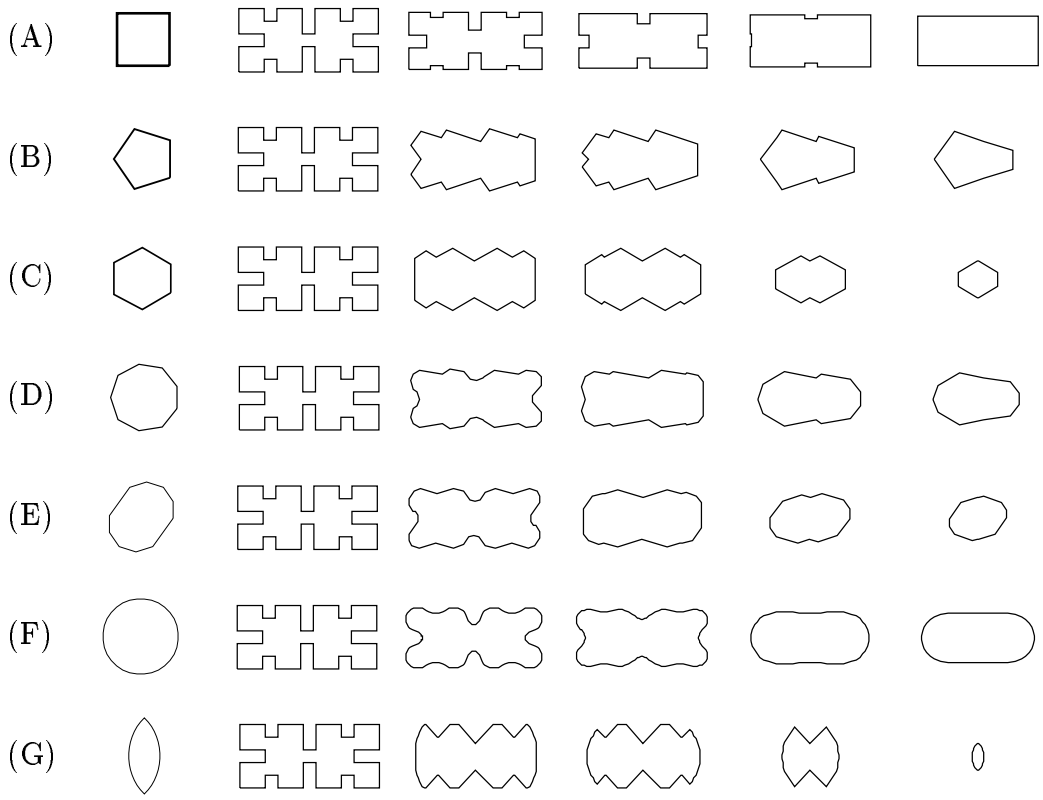

Fig. 9. Examples of the crystalline flow. The initial contour shown in the second column is common to all, and its evolution is shown from left to right. The Wulff shapes are shown in the left column: (A) a square, (B) a regular pentagon, (C) a regular hexagon, (D) a regular 9-polygon, (E) a 10-polygon which has two longer facets, (F) a regular 32-polygon, and (G) a 32-polygon in which each facet has same length.

4.2 Dominant Facet Extraction using a Crystalline Flow

As mentioned in Sec.1, a crystalline flow is useful for a multi-scale analysis of a contour figure. In the following, we will present a method that extracts several sets of dominant facets from a given polygon using a crystalline flow. Here, a dominant facet represents a large area of the given polygon in which the shape of the contour is approximately convex or concave. The presented method is analogous to classical multi-scale methods for corner extraction (see e.g. [5]). A convex (concave) corner is a local maximum (minimum) point of curvature in a contour. Those methods compute a curve shortening flow from a given contour, and extract dominant corners that are inherited for a long time interval in the evolving process. On the other hand, our method computes the crystalline flow, and extracts dominant facets that have non-zero transition number and have long lifetime in the evolving process.

In order to extract dominant facets from a given polygon, we make a scale-

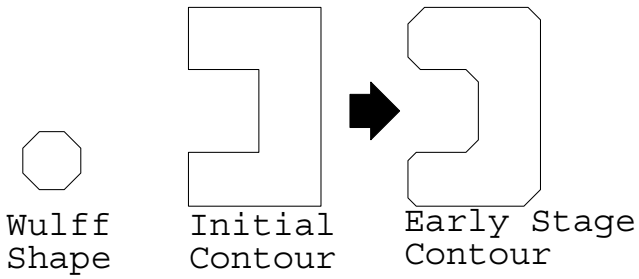

Fig. 10. An initial contour $S(0)$ and the corresponding early stage contour $S(\tilde{t})$

space representation[1] using the crystalline flow. Here, the x-axis of the scale-space shows the indices j of early stage contour defined below, and the y-axis shows the time t. Let us consider crystalline flow $S(t)$ starting from initial contour $S(0)$ which is a general simple polygon. As we mentioned in Sec.2, some facets may be created at some corners spontaneously, so that the initial polygon becomes essentially admissible right after $t = 0$. As time evolves, no more facets are created other than at $t = 0$; however, at most two consecutive facets with zero transition number may disappear[21].

We say that $S(\tilde{t})$ is an *early stage contour* if no facet disappears and no degenerate pinching and no selfintersection occurs for all $t \in (0, \tilde{t}]$ (see Fig.10). We index all facets of an early stage contour by $j = 1, 2, \cdots, r$, clockwisely. The totality of indices denotes $\mathcal{I}$; we consider this set modulo r. We shall correspond a subset $\mathcal{I}_h(t)$ of consecutive indices in $\mathcal{I}$ to each facet $F_h(t)$ of $S(t) = \cup_{h=1}^{k} F_h(t)$ and divide $\mathcal{I}$ into disjoint subsets $\{\mathcal{I}_h(t)\}_{h=1}^{k}$ in the following inductive way. We call $\mathcal{I}_h(t)$ the set of early stage indices of $F_h(t)$. Suppose that all sets of early stage indices of $S(t)$ are already known.

Suppose that $F_l(\tau)$ disappears at $t_1 > t$ and that no facets disappears at $s \in (t, t_1)$. Then, we set $\mathcal{I}_h(s) = \mathcal{I}_h(t)$ for $s \in (t, t_1)$. We shall construct the set of early stage indices at t_1 as follows. If both F_{l-1} and F_{l+1} do not disappear at t_1, then we add $\mathcal{I}_{l-1}(t)$, $\mathcal{I}_l(t)$, and $\mathcal{I}_{l+1}(t)$ to the set of early stage indices of a (merged) facet $F_*(t_1)$ containing the limit of $F_{l-1}(s)$ and $F_{l+1}(s)$ as $s \uparrow t_1$ (see Fig.11(A)). If F_{l-1} (resp. F_{l+1}) and F_l disappear at t_1, then we add $\mathcal{I}_l(t)$ to the set of early stage indices of a facet $F_*(t_1)$ containing the limit $F_{l+1}(s)$ (resp. $F_{l-1}(s)$) as $s \uparrow t_1$ (see Fig.11(B)).

By this procedure, the set of early stage indices is uniquely determined for each facet of $S(t)$ as far as $S(t)$ is essentially admissible. (Note that $\mathcal{I}$ is divided into sets of early stage indices at $t > 0$.) Different from Sec.2, one facet $F_h(t)$ may have several indices of $\mathcal{I}_h(t)$. Let $\chi(j, t)$ denote the transition number of the facet $F_h(t)$ such that $\mathcal{I}_h(t)$ contains j. As is shown in Fig.11, the transition number is plot at the corresponding position in the scale-space. This representation is analogous to a usual curvature scale-space.

Figure 12 presents an example of a crystalline flow numerically obtained with

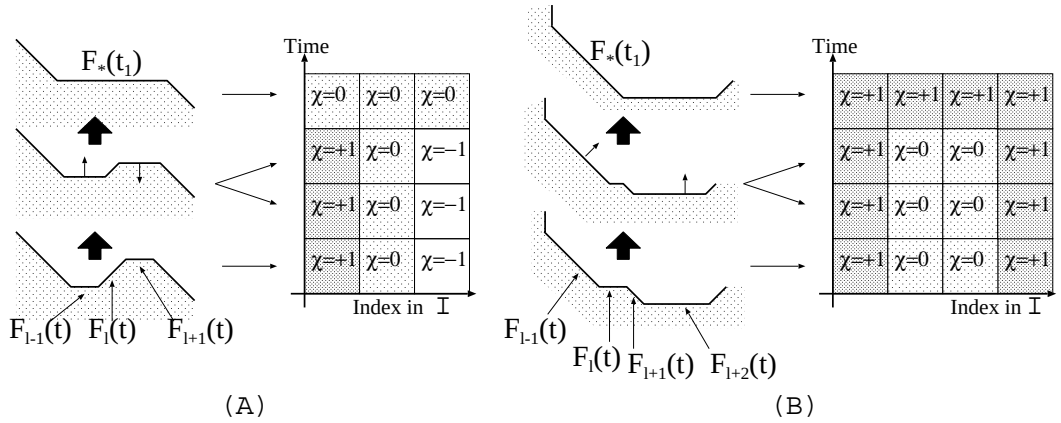

Fig. 11. A scale-space representation of the transition number. It is proved that, if $V = \Lambda_\gamma$, then all disappearing facet have zero transition number, and at most two consecutive facets disappear. The x-axis represents the index of facet in the early stage contour, and the y axis represents the time t.

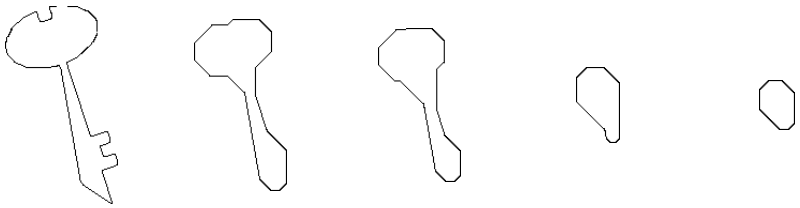

Fig. 12. An example of a crystalline flow. The Wulff shape is a regular octagon.

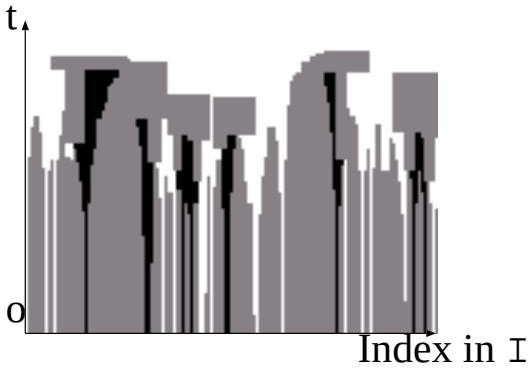

Fig. 13. The scale-space representation that corresponds to Fig.12. The white area represents $\chi_j = -1$, black one $\chi_j = +1$, and the gray one $\chi_j = 0$.

a regular octagon as a Wulff shape. As t increases, the number of (non-trivial) facets in an evolving contour decreases. The evolving polygon becomes an octagon in finite time. When the evolving contour becomes an octagon, the transition numbers of all facets become -1. Figure 13 shows the scale-space representation corresponds to the crystalline shown in Fig.12.

Referring to the scale-space representation of the transition number, we extract dominant facets whose transition numbers are not 0 and the values of the transition numbers are inherited for a long time interval in the evolving

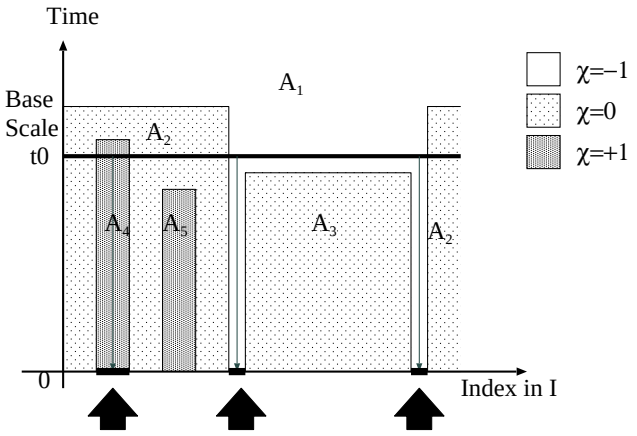

Fig. 14. Dominant facet extraction using the scale-space representation. The facets in an initial contour $\chi \neq 0$ are extracted, if they can be tracked to the base scale t_0.

process. Our algorithm is as followings.

(1) Make the scale-space representation of the transition number $\chi(j,t)$, where j is in $\mathcal{I}$ and t is the time.
(2) Divide the scale-space into areas, so that each area has the uniform value of $\chi(j,t)$ inside, and has different value from the neighboring areas. Let denote such the area as A_k, where $k = 1, 2, \cdots, n$ is the serial number.
(3) Set the base scale t_0, and draw a line $t = t_0$ in the scale space. Then, find a set of numbers $\mathcal{U}_{t_0}$, so that the area A_k contains the line $t = t_0$ and that $\chi(j,t) \neq 0$ on A_k, if $k \in \mathcal{U}_{t_0}$.
(4) Extract all indices from $\mathcal{I}$ (the set of all indices of early stage contour) that are included in the area $A_k(\tilde{t})$ for some $k \in \mathcal{U}_{t_0}$. Here, $A_k(\tilde{t})$ is the cross-section of A_k at the time $\tilde{t}$ at which $S(\tilde{t})$ is an early stage contour. We call facets of an early stage contour corresponding to such extracted indices *dominant facets* at t_0. Each of these indices corresponds to a facet of the early stage contour whose transition number is inherited to the evolving contour at t_0. In Fig.14, the indices of the dominant facets are indicated by up-arrows.
(5) Increase the base scale t_0 by small amount Δt, and repeat (3),(4), and (5), if t_0 is smaller than the scale at which the evolving contour becomes convex (provided that the evolving contour is essentially admissible).

We note that the set of all dominant facets may differ for different base scale t_0. If $t_0 < t_1$, then, $\mathcal{U}_{t_0} \supseteq \mathcal{U}_{t_1}$. As the result, the number of the dominant facets does not increase as t_0 increases.

Figure 15 shows the dominant facets. The early stage contour has 310 facets. By changing the base scale t_0, we obtain several sets of dominant facets. The approximations of a given contour are shown by linking the facets of early stage contour. As shown in Fig.15, fewer facets were extracted for higher value of the base scale. Figure 16 shows the graph of the number of dominant facets

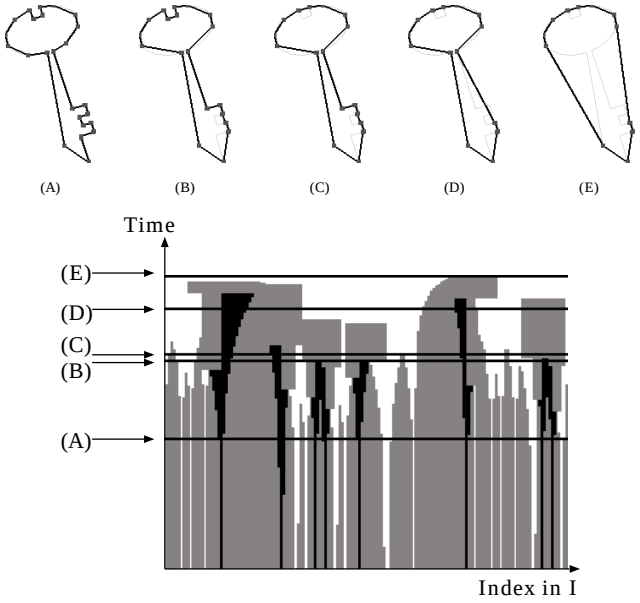

Fig. 15. An experimental result of dominant facet extraction. The corresponding base scales are shown with lines in the scale-space.

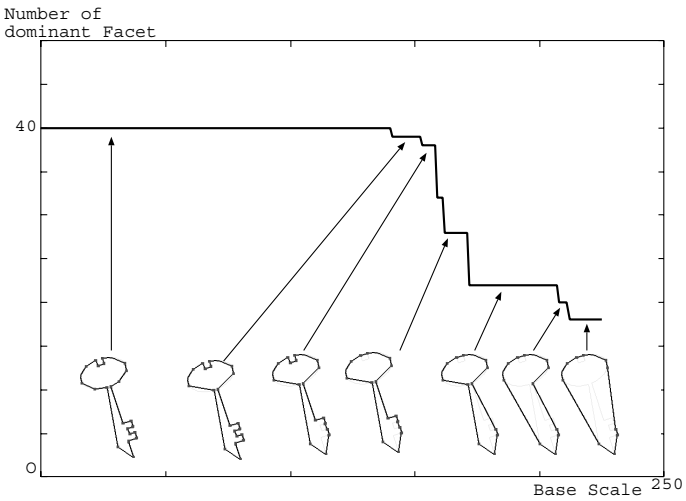

Fig. 16. The change of the dominant facets with respect to the base scale t_0.

with respect to the change of the base scale. The graph has a staircase pattern. The set of dominant facets which is stable with respect to the change of the base scale gives intuitively good result.

5 Conclusion

A numerical method for obtaining a crystalline flow starting from a given polygon that is not essentially admissible is presented. The method enables us to use any simple and convex polygon for the Wulff shape.

In many cases, a contour in an image is given as a polygon. For example, a contour represented with a chain-code is a polygon that consists of short facets. Because the nonlocal curvature Λ_γ is determined by the facet length, we can calculate the nonlocal curvature correctly. In addition, because each facet moves with keeping its direction, it is not difficult to track every facet through the evolving process. We show an application of a crystalline flow for the multi-scale analysis of a contour figure in an image. Tracking each facet of an evolving polygon, the method makes the scale-space representation from a given polygon, and extracts several sets of dominant facets. We believe that it is useful for a multi-scale analysis of a contour figure that any simple and convex polygon can be used for a Wulff shape.

References

[1] A. P. Witkin: Scale Space Filtering: A New Approach to Multi-Scale Descriptions, in Proceedings of 8th International Joint Conference of Artificial Intelligence (1983) 1019–1022

[2] J. J. Koenderink: The Structure of Images, Biological Cybernetics, **50** (1984) 363–370

[3] L. Alvarez and F. Guichard: Axioms and Fundamental Equations of Image Processing, Arch. Rational Mech. Anal., **123** (1993) 199–257

[4] F. Mokhtarian and A. Mackworth: A Theory of Multiscale, Curvature-Based Shape Representation for Planner Curves, IEEE Transactions on Pattern Analysis and Machine Intelligence, **14**, No.8 (1992) 789–805

[5] A. Rattarangsi and R. T. Chin: Scale-Based Detection of Corners of Planar Curves, IEEE Transactions on Pattern Analysis and Machine Intelligence, **14**, No.4 (1992) 430–449

[6] B. B. Kimia and A. R. Tannenbaum and S. W. Zucker: Shapes, Shocks, and Deformations I: The Components of Two-Dimensional Shape and the Reaction-Diffusion Space, International Journal of Computer Vision, **15** (1995) 189–224

[7] H. Hontani and K. Deguchi: Multi-Scale Image Analysis for Detection of Characteristic Component Figure Shapes and Sizes, Proceedings of 14th International Conference on Pattern Recognition (1998) 1470–1472

[8] S. Osher and J. A. Sethian, Fronts propagating with curvature-dependent speed: Algorithms based on Hamilton-Jacobi formulations, J. Comput. Phys. **79** (1988) 12–49

[9] L. C. Evans and J. Spruck, Motion of level-sets by mean curvature, I, J. Differential Geometry, **33** (1991) 635–681

[10] Y.-G. Chen, Y. Giga and S. Goto, Remarks on viscosity solutions for evolution equations, J. Differential Geometry, **33** (1991) 749–786

[11] S. B. Angenent and M. E. Gurtin, Multiphase thermomechanics with interfacial structure 2. Evolution of an isothermal interface, Arch. Rational Mech. Anal., **108** (1989) 323–391

[12] J. Taylor, Constructions and conjectures in crystalline nondifferential geometry, Proceedings of the Conference on Differential Geometry, **52**, Pitman, London (1991) 321–336

[13] M.-H. Giga and Y. Giga, Crystalline and level-set flow – Convergence of a crystalline algorithm for a general anisotropic curvature flow in the plane, Free boundary problems: theory and applications I (ed. N. Kenmochi) Gakuto International Ser. Math. Sci. Appl., **13** (2000) 64–79

[14] M.-H. Giga and Y. Giga, Generalized Motion by Nonlocal Curvature in the Plane, Arch. Rational Mech. Anal., **159** (2001) 295–333

[15] M.-H. Giga, Y. Giga and H. Hontani, Selfsimilar solutions in motion of curves by crystalline energy, Minisymposium lecture of 5th International Congress on Industrial and Applied Mathematics, Sydney, (2003) July

[16] H. Hontani, M.-H. Giga, Y. Giga, and K. Deguchi, A computation of a crystalline flow starting from non-admissible polygon using expanding selfsimilar solutions, 11th International Conference DGCI 2003, LNCS 2886, Springer, Naples, (2003) 465–474

[17] H. Hontani and K. Deguchi, Introducing a Crystalline Flow for a Contour Figure Analysis, IEICE Trans. (D) Information and System, Vol.E86-D, No.7, (2003) 1198–1205

[18] M. E. Gurtin, Thermomechanics of Evolving Phase Boundaries in the Plane, Oxford, Clarendon Press (1993)

[19] Y. Giga, A level set method for surface evolution equations, Sugaku 47 (1993) 321–340: Eng. translation, Sugaku Exposition **10** (1995), 217–241

[20] Y. Giga and S. Goto, Motion of hypersurfaces and geometric equations, J. Mathematical Society Japan, **44** (1992) 99–111

[21] M.-H. Giga and Y. Giga: Consistency in evolutions by crystalline curvature, Free Boundary Problems '95, Theory and Applications (eds. M. Niezgodka and P. Strzelecki), Proc. of the Zakopane Congress, Poland (1995) 186–202